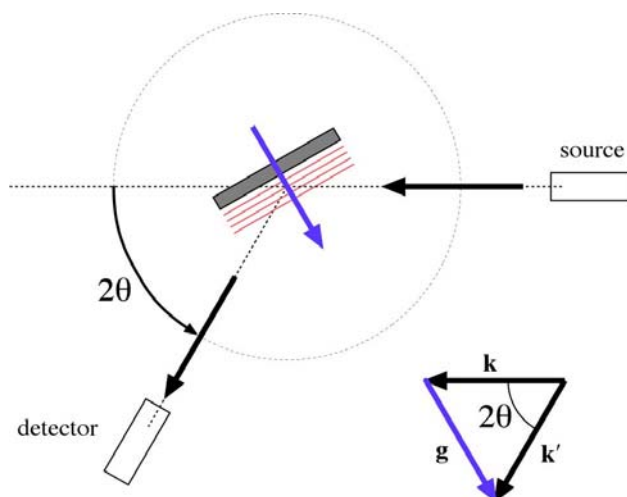


4. X-Ray Diffraction

X-ray diffraction geometry

A simple X-ray diffraction (XRD) experiment might be set up as shown below. We need a parallel X-ray source, which is usually an X-ray tube in a fixed position with optics to both collimate the beam and filter out only a narrow range of X-ray wavelengths. The X-ray beam diffracts off a sample, and the diffracted intensity is measured with a detector on the end of an arm that can rotate about the sample. The plane of diffraction contains the incident (wavevector \mathbf{k}) and diffracted (wavevector \mathbf{k}') X-ray beams. We must be able to rotate the sample so that the RLV of is interest is in the diffraction plane.

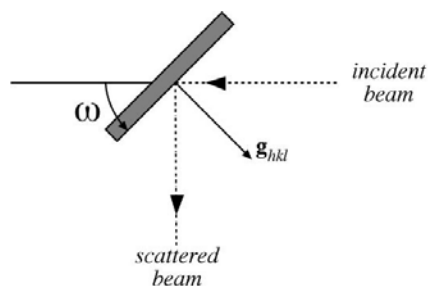


Often, we want to examine the diffraction from planes parallel to the substrate, i.e., having their \mathbf{g} vectors oriented along the substrate normal. In that case, as we scan through some range of 2θ with the detector, we must be simultaneously changing the sample orientation w.r.t. the incident beam to maintain $\mathbf{k}' - \mathbf{k} = \mathbf{g}$.

It is certainly possible to rotate the source, instead of the sample, but the source has high-voltage cables and water lines, whereas the sample is often small, so a fixed source is more common.

Setting ω

The motor that rotates the sample about an axis normal to the diffraction plane is called ω (or Ω).



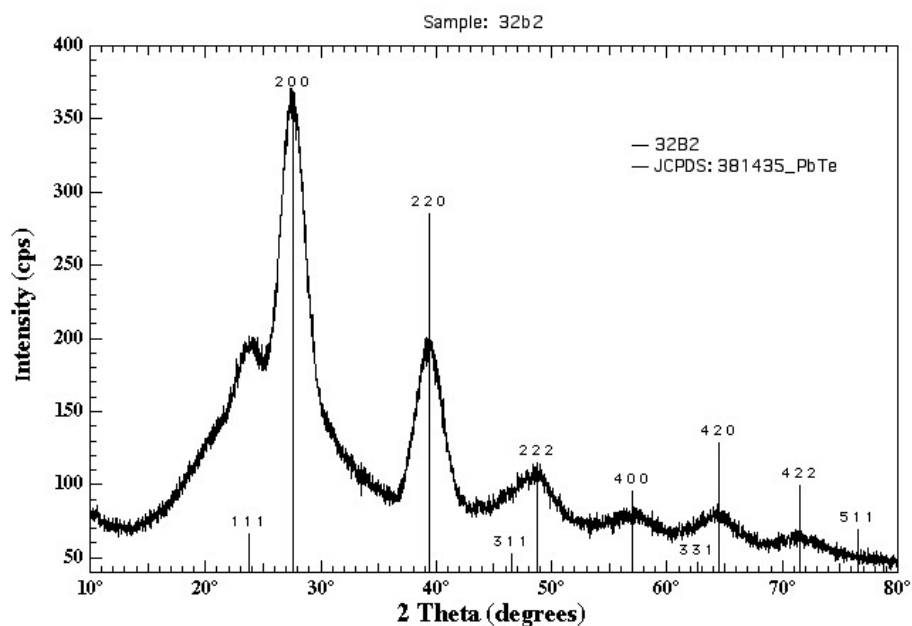
It has an especially important role for films. We usually mount the substrate so that its plane is parallel to the beam axis and normal to the diffraction plane when $\omega = 0$. Then, if want to scan along the normal to the substrate plane, we set

$$\omega = \frac{1}{2}(2\theta) = \theta$$

In this case, ω and θ are basically synonymous.

X-ray diffraction patterns from nanoparticles

Powder diffraction is a way to analyze a material by grinding it up into many small particles that are randomly oriented. But we may refer to the diffraction pattern from a collection of nanoparticles, or even a polycrystalline material, as a powder pattern. Powder patterns are simple to analyze, because there is no dependence on specimen orientation; every orientation is represented in the data. So standard patterns are recorded for comparison to any arbitrary test sample. An example of a powder pattern from PbTe nanoparticles is shown below.



There are a few things to notice. The most important is the positions of the peaks. We can identify their Miller indices once we have found the correct standard (vertical lines) for comparison. But some attention should be given to the relative peak heights. It is very uncommon to be able to quantitatively explain the absolute peak heights, but the relative heights should be a fairly close match. This is especially true for real powders, when the particle size is larger than a few microns. When comparing nanoparticles to a powder standard (as in the example above) we should allow some differences due to the particular particle shapes.

Another feature we should notice above is the peak widths. This sample contained very small particles, only a few nm in diameter, which causes a very broad peaks, more than $1-2^\circ$ in 2θ . For a large-grained powder, the peaks may be quite narrow. In that case, the peak widths are mainly determined by the XRD instrument, rather than the sample.

Powder-diffraction standards

The most common database of powder diffraction standards is managed by the Joint Committee on powder Diffraction Standards (JCPDS), which is associated with the International Union of

Crystallography & Structure of Nanomaterials

Crystallography. Each particular standard is saved in a powder diffraction file (PDF). These standard files are interchangeably called JCPDS files or PDFs. A portion of an example is shown below:

```

PDF#00-029-1360: QM=Star(S); d=(Unknown); I=Diffractometer
Brookite
TiO2      Black
Radiation=CuKa1  Lambda=1.54056  Filter=Ni
Calibration=      2T=25.340-103.201  I/Ic(RIR)=
Ref: Natl. Bur. Stand. (U.S.) Monogr. 25, v3 p57 (1964)

Orthorhombic - Powder Diffraction, Pcab (61)      Z=8      mp=
CELL: 5.4558 x 9.1819 x 5.1429 <90.0 x 90.0 x 90.0>  P.S.=oP24 (O2 Ti)
Density(c)=4.120  Density(m)=4.140  Mwt=79.90      Vol=257.63      F(30)=57.8(0115,45/0)
Ref: Ibid.

Strong Lines: 3.46/8 2.90/9 2.48/3 2.41/2 2.37/1
NOTE: To replace 00-016-0617 and validated by calculated pattern.
See ICSD 36408 (PDF 01-076-1934).
Specimen from Magnet Cove, Arkansas, USA (USNM 97661).
Spectrographic analysis: 0.1-1.0% Si; 0.01-0.1% each of Al, Fe, and V; 0.001-0.01% Mg.
Niobian brookite from Mozambique [Chemical analysis (wt.%): Ti O2 80.7, Nb2 O5 14.1, FeO 5.53];
Carvalho et al., Rev. Cien.Geol.Ser. A, 7 61 (1974) reports an identical pattern.
Pattern taken at 25 C.
Intensities verified by calculated pattern.

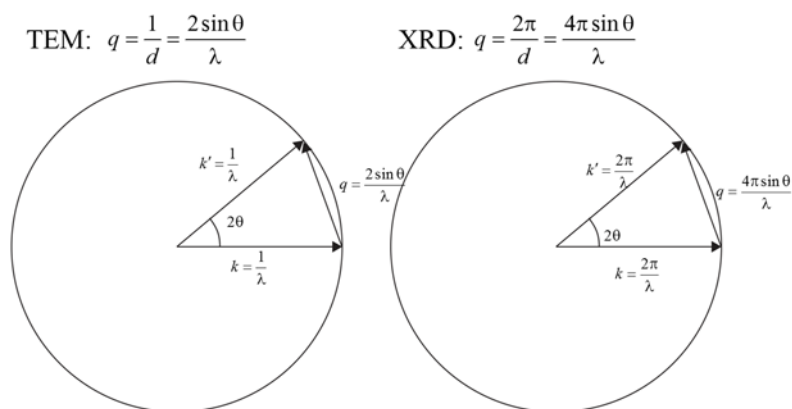
2-Theta  d(nm)  I(v)  (h k l)  Theta  1/(2d)  2pi/d n^2
25.340  0.35120  92.0  (1 2 0)  12.670  0.01424  0.17891
25.689  0.34650  74.0  (1 1 1)  12.845  0.01443  0.18133
30.807  0.29000  100.0  (1 2 1)  15.404  0.01724  0.21666
32.791  0.27290  5.0  (2 0 0)  16.395  0.01832  0.23024
36.252  0.24760  33.0  (0 1 2)  18.126  0.02019  0.25376
37.296  0.24090  24.0  (2 0 1)  18.648  0.02076  0.26082
37.933  0.23700  8.0  (1 3 1)  18.967  0.02110  0.26511
38.371  0.23440  5.0  (2 2 0)  19.185  0.02133  0.26805
38.576  0.23320  6.0  (2 1 1)  19.288  0.02144  0.26943
39.205  0.22960  7.0  (0 4 0)  19.603  0.02178  0.27366
39.967  0.22540  11.0  (1 1 2)  19.983  0.02218  0.27876
40.152  0.22440  26.0  (0 2 2)  20.076  0.02228  0.28000
42.339  0.21330  24.0  (2 2 1)  21.170  0.02344  0.29457
46.072  0.19685  26.0  (0 3 2)  23.036  0.02540  0.31919

```

The file is assigned a unique number, contains a name for the material, and some information about how the data was acquired. Then there is information about the physical properties, including the crystallographic space group and unit-cell dimensions. There are then some comments about the origins of the specimen. Last is a listing of the peak positions and/or d spacings, relative intensities (in %), and Miller indices.

Two conventions for scattering vector

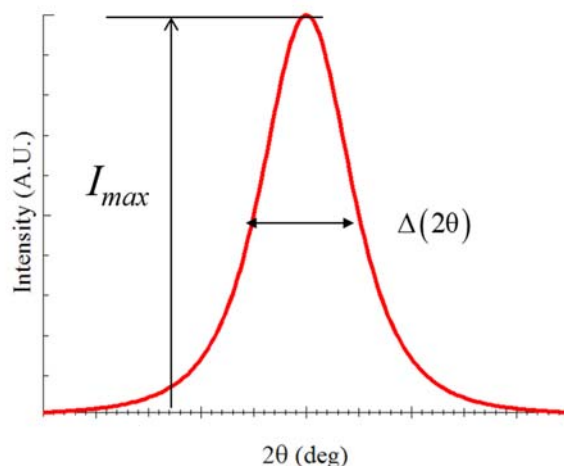
In the discussion of electron diffraction, the lengths of reciprocal-space vectors were always the inverse of a corresponding distance, such as a wavelength or d -spacing. In XRD, it is more common to include a factor of 2π when defining wavevector. The difference is whether the 2π is written explicitly in the exponent of a complex exponential, or whether it is included in the wavenumber.



The point is simply that I may slip between the two conventions inadvertently. Please bear with me.

Integrated intensity factors for powder

There is more than one way to express the intensity of a diffraction peak. The number of counts per unit area per unit time is the *absolute* intensity. What we actually measure is the total number over some finite area of detector per unit time. The total number per unit time integrated over the full range of the peak in 2π is called the *integrated* intensity. The integrated intensity in powder diffraction is proportional to a number of factors that we will list later.



The peak can have various shapes. Assuming all of the peak shapes are the same (with just different parameters) we could express the integrated intensity as:

$$I_{\text{int}} \propto I_{\text{max}} \cdot \Delta(2\theta)$$

where $\Delta(2\theta)$ is the width in 2θ .

Peak fitting

One way to extract parameters such as maximum intensity I_{max} and width $\Delta(2\theta)$ is by least-squares curve fitting. This requires an expected curve shape that depends on a few parameters, which can be varied until the squared difference between the data and fit function at each point is minimized. In practice, each data point is usually weighted by its uncertainty.

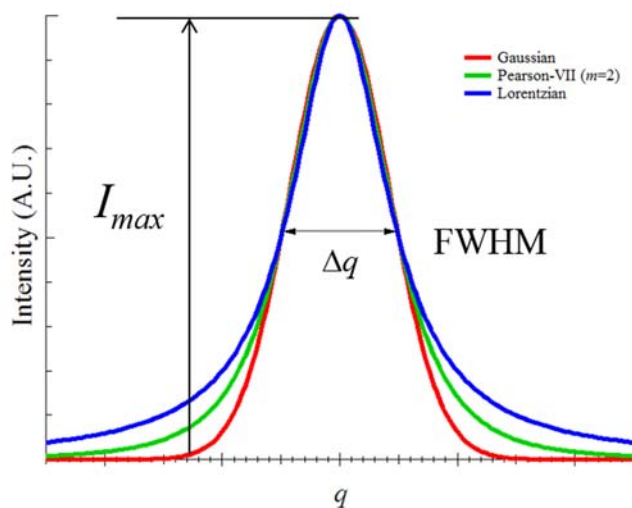
It is sometimes preferable to plot the data as a function of q , instead of 2θ . The centroid is q_0 and the width is Δq . Some common functions to use are listed below:

$$f_{\{q_0, \Delta q\}}^{\text{Gaussian}}(q) = \exp\left\{-\ln(2) \left[\frac{q - q_0}{(\Delta q/2)}\right]^2\right\}, // \text{gaussian}$$

$$f_{\{q_0, \Delta q\}}^{\text{Lorentzian}}(q) = \frac{1}{1 + \left[\frac{q - q_0}{(\Delta q/2)}\right]^2}, // \text{lortenzian}$$

$$f_{\{q_0, \Delta q, m\}}^{\text{Pearson-7}}(q) = \frac{1}{\left[1 + (2^{1/m} - 1) \cdot \left[\frac{q - q_0}{(\Delta q/2)}\right]^2\right]^m}, //\text{pearson-7}$$

We have arranged these in each case so that the width parameter Δq precisely the full width at half maximum (FWHM) of the peak, which is a standard metric. Note that the peaks are all normalized for maximum value of unity, but the the integrated intensities are not generally the same.



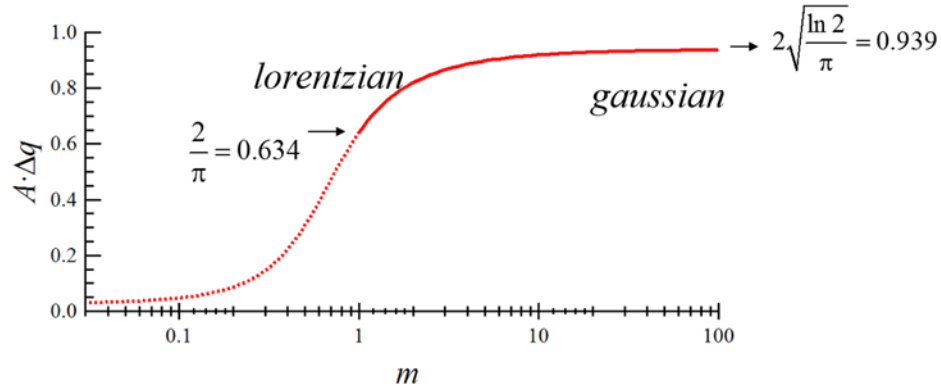
The gaussian shape is used throughout statistics and physics. It is often called a normal distribution, and represents the probability distribution when a quantity has a definite mean.

The lorentzian shape is unusual because it has no mean or standard deviation. Nonetheless, it does have a well-defined centroid (which corresponds to the median) and a FWHM.

The pearson-7 shape is a purely mathematical construct that makes it easy to vary between gaussian and lorentzian shapes. Notice the extra parameter, m . If $m=1$, we get the lorentzian shape. If $m \rightarrow \infty$, we get the gaussian shape. There is no such correspondence for $m < 1$, but we don't always care if the peak assume any particular, theoretical shape, especially if all we need to know is the peak position.

Normalization

In these forms, these peaks are normalized w.r.t. I_{max} , not integrated intensity. But the areas under the curves are not all the same.



Another important lineshape

The voigt function is defined as the convolution of a gaussian and a lorentzian centered at the same point q_0 , i.e.:

$$f_{\{q_0, \Delta q\}}^{\text{Voigt}}(q) = f_{\{q_0, \Delta q_1\}}^{\text{Gaussian}}(q) * f_{\{q_0, \Delta q_2\}}^{\text{Lorentzian}}(q)$$

It turns out that, since the gaussian and lorentzian are normalized, the voigt will be, too. The centroid q_0 doesn't change, but, because of the lorentzian component, the voigt has no well-defined mean or standard deviation. There is no simple expression for the FWHM Δq as a functions of Δq_1 and Δq_2 , but we know Δq will be larger than both Δq_1 and Δq_2 .

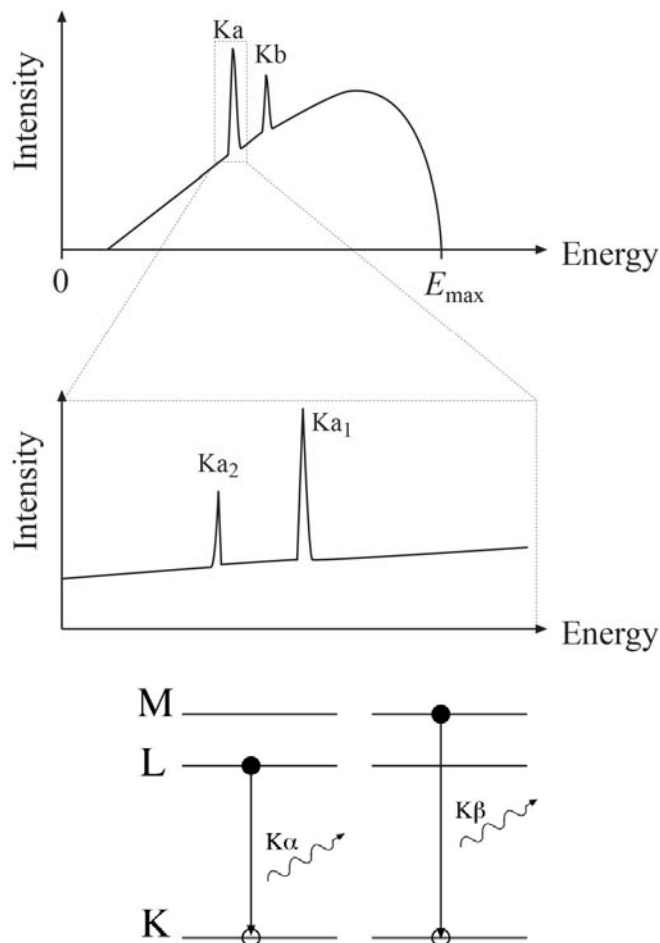
Sometime people use a pseudovoigt function, which is taken as a linear combination of a gaussian and a lorentzian, i.e.:

$$f_{\{q_0, \Delta q\}}^{\text{Pseudovoigt}}(q) = (1 - \eta) \cdot f_{\{q_0, \Delta q_1\}}^{\text{Gaussian}}(q) + \eta \cdot f_{\{q_0, \Delta q_2\}}^{\text{Lorentzian}}(q)$$

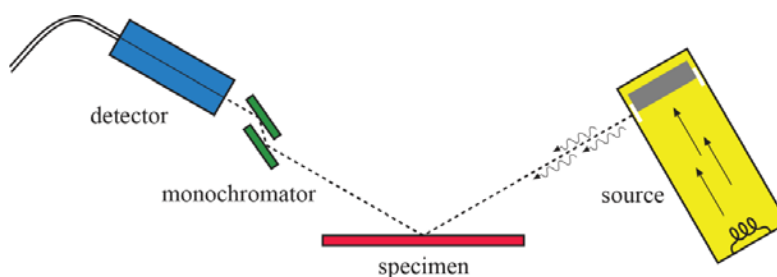
This is definitely easier to analyze, though the physical basis is shaky. We know the centroid remains q_0 , and if $\Delta q_1 = \Delta q_2 = \Delta q$, the FWHM will remain Δq . But the pseudovoigt really only approximates a voigt for certain combinations of Δq_1 , Δq_2 , and η .

X-ray sources

We know that ionization results in characteristic X-ray emission, while acceleration of electrons results in bremsstrahlung X rays. When we expose a target to an electron beam, both contributions will be present in the spectrum. There are two $K\alpha$ lines and one $K\beta$ line. For X-rays sources, we usually want to use the intensity of the K lines.



The most common type of X-ray source in laboratories is an X-ray tube. Inside the tube is a stationary metal target (usually Cu). When the source is on, the target is exposed to a beam of electrons from a filament, usually with around 40 kV accelerating potential. There are windows in the tube from which the X-ray beam escapes and is directed onto a specimen.



The scattered electron intensity is measured by a detector. Usually, there is a monochromator somewhere between the source and detector to remove most of the continuous bremsstrahlung spectrum, as well as the $K\beta$. But it is also possible to use a thin metal filter, such as Ni, which has an X-ray absorption spectrum that blocks the $K\beta$ and other unwanted X-ray energies. It is difficult to filter out the $K\alpha_2$, so it is often present in the resulting diffraction patterns.

The diffraction plane can be horizontal or vertical (or something else), but there needs to be freedom to move the specimen and detector w.r.t the incident beam. There are a variety of ways to do that.

Common X-ray sources

By far, the most common X-ray target used is Cu, with the alignment set so that the radiation used is Cu- $K\alpha$, but Mo- $K\alpha$ is not too uncommon.

target: Cu				
label	transition	E (KeV)	λ (nm)	relative intensity
$K\alpha_1$	$2p_{3/2} \rightarrow 1s$	8.048	0.15405	2.0
$K\alpha_2$	$2p_{1/2} \rightarrow 1s$	8.028	0.15443	1.0
			λ_{mean} (nm)	0.1542

target: Mo				
label	transition	E (KeV)	λ (nm)	relative intensity
$K\alpha_1$	$2p_{3/2} \rightarrow 1s$	17.481	0.07093	2.0
$K\alpha_2$	$2p_{1/2} \rightarrow 1s$	17.376	0.07135	1.0
			λ_{mean} (nm)	0.07107

The relative intensities of $K\alpha_1$ and $K\alpha_2$ are fixed at 2:1 by the multiplicities of the initial states involved. Because they are so close in wavelength, it is common to take a weighted sum as a reasonable estimation of the wavelength, when both are present.

Recall that, as photons, the energy-wavelength relationship is given by:

$$E = \frac{1240 \text{ eV} \cdot \text{nm}}{\lambda} = \frac{1.24 \text{ KeV} \cdot \text{nm}}{\lambda}$$

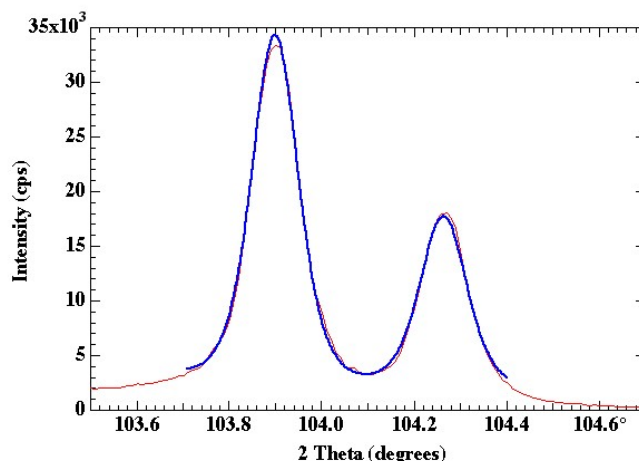
There are other targets available too, such as Co and Ag.

 $K\alpha$ peak doublets

Using $K\alpha$ radiation, it is unusual to completely filter out the $K\alpha_2$, so one is left with a doublet of closely spaced peaks. These are evident at high scattering angles. If there is no filtering of the $K\alpha_2$, we know that the relative intensity is precisely $I_{K\alpha_1}/I_{K\alpha_2} \approx 2.0$. These two peaks in 2θ can be thought of as one peak in q that correspond to a single lattice spacing. The θ values are related by

$$q = \frac{2\pi}{d} = \frac{4\pi \sin \theta_1}{\lambda_1} = \frac{4\pi \sin \theta_2}{\lambda_2}$$

So the two peaks should not be fit independently, as the relative positions and relative intensities are fixed.



Fitting the $K\alpha$ doublet

I would recommend fitting the peaks with something of the form

$$I(2\theta) = A_1 \cdot f_{\{q_0, \Delta q, \dots\}} \left(\frac{2 \sin \theta}{\lambda_1} \right) + A_2 \cdot f_{\{q_0, \Delta q, \dots\}} \left(\frac{2 \sin \theta}{\lambda_2} \right) + b_0 + b_1 \cdot (2\theta) + b_2 \cdot (2\theta)^2$$

Essentially, the argument of the fitting functions is $q = 2 \sin \theta / \lambda$, where a different wavelength is used for each peak. But the centroids and FWHMs in q are the same, and amplitudes are fixed at 2:1.

X-ray scattering by charges

An electric charge in an electric field experiences a force

$$\mathbf{F} = q\mathbf{E}$$

A mass subjected to a force accelerates

$$\mathbf{a} = \mathbf{F}/m$$

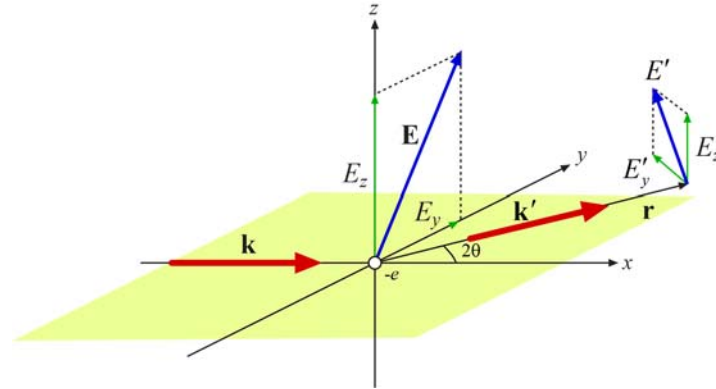
We know a stationary electric charge has an electric field around it. There is an additional component to the electric field when the charge is accelerating. This is what gives rise to bremsstrahlung. If a charge at the origin is at rest, but has acceleration \mathbf{a} , the additional electric field at position \mathbf{r} is

$$\mathbf{E}' = \frac{q}{c^2 r^3} \cdot [\mathbf{r} \times (\mathbf{r} \times \mathbf{a})]$$

When X rays scatter off of electric charges in materials, the electrons accelerate due to the sinusoidal electric field of the incident electromagnetic wave. Because of this oscillatory motion, the electrons then reradiate at the same frequency as the incident field, such that the strength of the electric field varies as in the above equation. This is all we need to know to predict the variation in scattered intensity with respect to the incident X-ray beam direction.

X-ray scattering from one electron

Imagine an X-ray beam parallel to the x-axis and an electron ($q = -e$) located at the origin.



Electromagnetic radiation (light) consists of transverse waves, so the electric field of the incident beam can have a y component E_y and a z component E_z . Let's find the electric field components of the scattered wave at an observation point in the x - y plane at an angle 2θ w.r.t. the x -axis. Applying the preceding double cross product, we find that the resulting components of the scattered wave are

$$E'_y = \frac{e^2 E_y}{mc^2 r} \cos(2\theta) \quad \text{and} \quad E'_z = \frac{e^2 E_z}{mc^2 r}$$

There is no coupling between y and z components; they are completely independent. Only E'_y has a dependence on scattering angle. Notice that E'_y vanishes at $2\theta = 90^\circ$, so any scattered X rays at right angles from the incident beam are completely polarized.

The X-ray intensity is proportional to the magnitude squared of the electric field. For the incident and scattered beams

$$I \propto |E|^2 \quad \text{and} \quad I' \propto |E'|^2$$

If we don't distinguish polarization, the total magnitude squared of the electric field is the sum of y and z components

$$|E|^2 = |E_y|^2 + |E_z|^2$$

$$|E'|^2 = |E'_y|^2 + |E'_z|^2 = \frac{e^4}{(mc^2)^2 r^2} (|E_y|^2 \cos^2(2\theta) + |E_z|^2)$$

Polarization factor

When we are measuring intensities, we are really only concerned with the time-averaged electric fields, not the sinusoidal part, i.e.

$$\langle |E|^2 \rangle = \langle |E_y|^2 \rangle + \langle |E_z|^2 \rangle$$

If the incident beam is unpolarized, then

$$\langle |E_y|^2 \rangle = \langle |E_z|^2 \rangle = \frac{1}{2} \langle |E|^2 \rangle$$

We can see that

$$\langle |E'|^2 \rangle = \frac{e^4}{(mc^2)^2 r^2} [\cos^2(2\theta) + 1] \langle |E|^2 \rangle$$

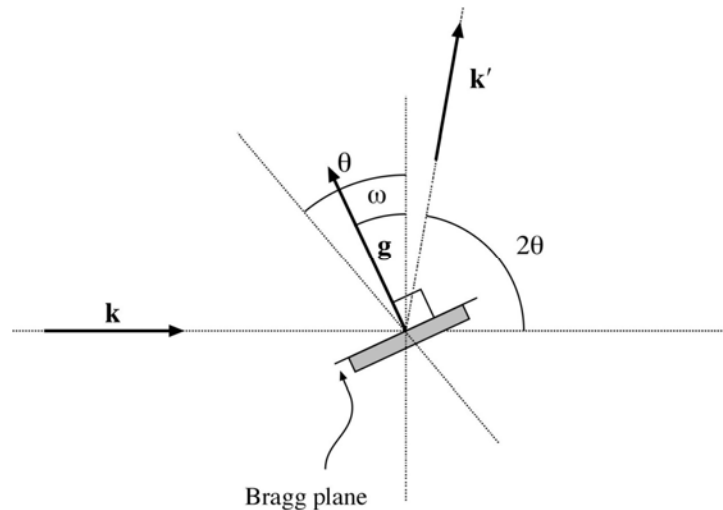
We will just say

$$I' = \frac{e^4}{(mc^2)^2 r^2} \left(\frac{\cos^2(2\theta) + 1}{2} \right) \cdot I$$

The term in square brackets is the polarization factor that gives the variation in scattered X-ray intensity with scattering angle when the incident beam is unpolarized. (If the beam is polarized the separate y and z factors will need to be mixed appropriately. Most X-ray tube sources are not polarized, but some sources, such as an X-ray synchrotron source, may have varying degrees of polarization.)

Diffraction geometry

We need to define coordinates to specify the sample orientation whether or not it is at the Bragg condition. We use ω as the mechanical angle that rotates the sample. The mechanical angle that controls the detector position is 2θ . The angle θ is really an abstraction that is half of 2θ . It is sufficient to assume the \mathbf{g} of interest is already in the diffraction plane (containing \mathbf{k} and \mathbf{k}'). (For single crystals, this may involve other mechanical angles, which we will discuss later. The emphasis here is powders.) In the context of powder diffraction, we almost always assume $\mathbf{g} \perp \mathbf{k}$ when $\omega = 0$.



Excitation error in XRD (I)

Recall the excitation error, a measure of deviation from the Bragg condition. Its length is the distance from a reciprocal-lattice point to the Ewald sphere.

$$\mathbf{s} = \mathbf{k}' - \mathbf{k} - \mathbf{g}$$

Let us specify these vectors using the established coordinate system

$$\mathbf{k} = k\hat{\mathbf{x}}$$

$$\mathbf{k}' = k \cdot [\cos(2\theta)\hat{\mathbf{x}} + \sin(2\theta)\hat{\mathbf{y}}]$$

$$\mathbf{g} = g \cdot (-\sin\omega\hat{\mathbf{x}} + \cos\omega\hat{\mathbf{y}})$$

Recall that 2θ is the detector angle and ω is the sample rotation in the diffraction plane.

Excitation error in XRD (II)

We need to know the difference

$$\begin{aligned} \mathbf{k}' - \mathbf{k} &= k \{ [\cos(2\theta) - 1]\hat{\mathbf{x}} + \sin(2\theta)\hat{\mathbf{y}} \} \\ &= 2k \sin\theta \cdot (-\sin\theta \cdot \hat{\mathbf{x}} + \cos\theta \cdot \hat{\mathbf{y}}) \end{aligned}$$

Now we pick coordinates that move with sample:

$$\begin{aligned} \hat{\mathbf{x}}' &= -\sin\omega\hat{\mathbf{x}} + \cos\omega\hat{\mathbf{y}} & \hat{\mathbf{x}} &= -\sin\omega\hat{\mathbf{x}}' - \cos\omega\hat{\mathbf{y}}' \\ \hat{\mathbf{y}}' &= -\cos\omega\hat{\mathbf{x}} - \sin\omega\hat{\mathbf{y}} & \hat{\mathbf{y}} &= \cos\omega\hat{\mathbf{x}}' - \sin\omega\hat{\mathbf{y}}' \end{aligned}$$

In the new coordinates

$$\begin{aligned} \mathbf{k}' - \mathbf{k} &= 2k \sin(\theta) \cdot [\cos(\theta - \omega)\mathbf{x}' + \sin(\theta - \omega)\hat{\mathbf{y}}'] \\ \mathbf{g} &= g\mathbf{x}' \end{aligned}$$

In the sample coordinates, the excitation error is

$$\mathbf{s} = 2k \sin(\theta) \cdot [\cos(\omega - \theta)\hat{\mathbf{x}}' - \sin(\omega - \theta)\hat{\mathbf{y}}'] - g\hat{\mathbf{x}}'$$

Excitation error in XRD (II)

In the sample coordinates, \mathbf{s} depends on the angle $\omega_{\text{rel}} = \omega - \theta$

$$\mathbf{s} = 2k \sin\theta \cdot (\cos\omega_{\text{rel}} \cdot \hat{\mathbf{x}}' - \sin\omega_{\text{rel}} \cdot \hat{\mathbf{y}}') - g\hat{\mathbf{x}}'$$

For a radial scan, $\omega_{\text{rel}} = 0$, so

$$\mathbf{s} = (2k \sin\theta - g) \cdot \hat{\mathbf{x}}'$$

Notice that, if $s = 0$, then

$$\sin\theta = \frac{g}{2k}$$

In other words, $\theta = \theta_B$ at the Bragg condition, as expected.

Geometric factor (Ia)

We saw that the reciprocal lattice points of a small crystal are broadened in reciprocal space. We can imagine integrating the scattering strength over the peak in reciprocal space, where the relevant coordinates are those of the excitation error vector \mathbf{s} in the diffraction plane:

$$I_{\text{int}}^{(s)} \propto \int_{s_x, s_y} S(s_x, s_y) \cdot ds_x \cdot ds_y$$

But, experimentally, we integrate over an angular range:

$$I_{\text{int}}^{(\theta)} \propto \int_{\omega_{\text{rel}}, \theta} S(s_x, s_y) \cdot d\omega_{\text{rel}} \cdot d\theta$$

The integral over ω_{rel} occurs when a powder is used. The integral over θ occurs when we are integrating over a range of 2θ . We could write the scattering strength at some vector \mathbf{s} as

$$S(s_x, s_y) = \int_{s'_x, s'_y} S(s_x - s'_x, s_y - s'_y) \cdot \Delta(s'_x) \cdot \Delta(s'_y) \cdot ds'_x \cdot ds'_y$$

The integrated intensity is then

$$I_{\text{int}}^{(\theta)} \propto \int_{s'_x, s'_y} \left[\int_{\omega_{\text{rel}}, \theta} S(s_x - s'_x, s_y - s'_y) \cdot d\omega_{\text{rel}} \cdot d\theta \right] \cdot \Delta(s'_x) \cdot \Delta(s'_y) \cdot ds'_x \cdot ds'_y$$

Lorentz-polarization factor

For a powder pattern, using unpolarized X rays, a variety of intensity contributions related to the scattering geometry should be considered. These are often combined into a single term, called the Lorentz-polarization factor

$$L(\theta_B) = \cos(\theta_B) \cdot \frac{1}{\sin(2\theta_B)} \cdot \frac{1}{\sin(2\theta_B)} \cdot [1 + \cos^2(2\theta_B)] = \frac{1 + \cos^2(2\theta_B)}{\sin(\theta_B) \cdot \sin(2\theta_B)}$$

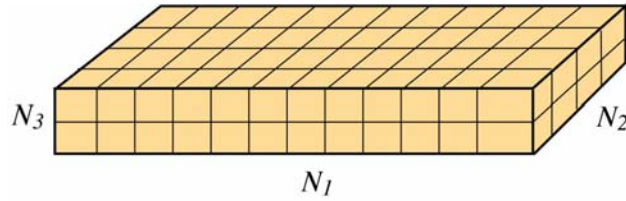
All of the diffracted intensities will be weighted by this factor. But there are other factors, too. There is a multiplicity factor m for powders, because symmetry equivalent planes will superpose in the diffracted intensity. This is the number of equivalent permutations of Miller indices that correspond to a particular reflection. For example, a cubic crystal has 8 types of $\{111\}$ planes and 12 types of $\{220\}$ planes. Since the orientation of a powder is completely random, any of these permutations can contribute to a particular peak. Powder X-ray diffraction is almost completely kinematical diffraction, so the intensities vary as structure-factor squared. We also saw this in electron diffraction, we just evaluate it a little differently for X rays, compared to electrons.

$$I \propto m \cdot |F|^2 \cdot L(\theta_B) \cdot M(\theta_B, T)$$

We also have included the Lorentz-polarization factor and the Debye-Waller, or thermal, factors $M(\theta_B, T)$, which accounts for the damping of scattering power for large-angle reflections due to crystal vibrations.

Scattering from a small crystal

Assume our specimen is a small crystal with a rectangular parallelepiped shape, made of N_1 , N_2 , and N_3 cubic unit cells parallel to basis vectors \mathbf{a}_1 , \mathbf{a}_2 , and \mathbf{a}_3 , respectively.



If the scattering amplitude from each unit cell is F , the total scattering amplitude with incident and scattered wave vectors \mathbf{k} and \mathbf{k}' is

$$E \propto F \sum_{n_1=0}^{N_1-1} e^{2\pi i n_1 (\mathbf{k}' - \mathbf{k}) \cdot \mathbf{a}_1} \cdot \sum_{n_2=0}^{N_2-1} e^{2\pi i n_2 (\mathbf{k}' - \mathbf{k}) \cdot \mathbf{a}_2} \cdot \sum_{n_3=0}^{N_3-1} e^{2\pi i n_3 (\mathbf{k}' - \mathbf{k}) \cdot \mathbf{a}_3}$$

There is a trick credited to Gauss for performing these sums:

$$S = \sum_{n=0}^{N-1} x^n = 1 + x^1 + x^2 + \dots + x^{N-1}$$

$$xS = \sum_{n=0}^{N-1} x^{n+1} = x^1 + x^2 + \dots + x^N$$

$$S = \frac{1 - x^N}{1 - x}$$

So

$$\left| \frac{1 - e^{2\pi i N (\mathbf{k}' - \mathbf{k}) \cdot \mathbf{a}}}{1 - e^{2\pi i (\mathbf{k}' - \mathbf{k}) \cdot \mathbf{a}}} \right|^2 = \left\{ \frac{\sin [\pi N (\mathbf{k}' - \mathbf{k}) \cdot \mathbf{a}]}{\sin [\pi (\mathbf{k}' - \mathbf{k}) \cdot \mathbf{a}]} \right\}^2$$

Now the combined intensity is

$$I \propto |F|^2 \left\{ \frac{\sin [\pi N_1 (\mathbf{k}' - \mathbf{k}) \cdot \mathbf{a}_1]}{\sin [\pi (\mathbf{k}' - \mathbf{k}) \cdot \mathbf{a}_1]} \right\}^2 \cdot \left\{ \frac{\sin [\pi N_2 (\mathbf{k}' - \mathbf{k}) \cdot \mathbf{a}_2]}{\sin [\pi (\mathbf{k}' - \mathbf{k}) \cdot \mathbf{a}_2]} \right\}^2 \cdot \left\{ \frac{\sin [\pi N_3 (\mathbf{k}' - \mathbf{k}) \cdot \mathbf{a}_3]}{\sin [\pi (\mathbf{k}' - \mathbf{k}) \cdot \mathbf{a}_3]} \right\}^2$$

Small crystal ↔ thin foil

Remember the kinematical theory of electron diffraction applied to a thin foil? We found

$$I_{\mathbf{g}} = \frac{(\pi T)^2}{|\xi|^2} \cdot \text{sinc}^2(\pi s T) = \left(\frac{\lambda T}{v} \right)^2 \cdot |F|^2 \text{sinc}^2(\pi s T)$$

where the second form is written in terms of structure factor, instead of extinction distance. Consider the formulation in the preceding section, assuming there is only one small axis that we are interested in. We know that $\mathbf{g} \cdot \mathbf{a} = n \in \mathcal{C}$, Writing $\mathbf{k}' = \mathbf{k} + \mathbf{g} + \mathbf{s}$, we know that

$$(\mathbf{k}' - \mathbf{k}) \cdot \mathbf{a} = (\mathbf{g} + \mathbf{s}) \cdot \mathbf{a} = n + \mathbf{s} \cdot \mathbf{a}$$

Now we have

$$I \propto |F|^2 \left[\frac{\sin(\pi N \mathbf{s} \cdot \mathbf{a})}{\sin(\pi \mathbf{s} \cdot \mathbf{a})} \right]^2$$

If we are not too far from the Bragg condition, then $\sin(\pi \mathbf{s} \cdot \mathbf{a}) \approx \pi \mathbf{s} \cdot \mathbf{a}$. Now

$$I \propto |F|^2 \left[\frac{\sin(\pi N \mathbf{s} \cdot \mathbf{a})}{\sin(\pi \mathbf{s} \cdot \mathbf{a})} \right]^2 = N^2 |F|^2 \text{sinc}^2(\pi N \mathbf{s} \cdot \mathbf{a})$$

This has the same form as the TEM result, other than some constant factors, and substituting $T = Na$. Instead of T^2 , we now have N^2 .

Approximation

If we are near the Bragg condition (small s), a reasonable approximation is

$$\text{sinc}^2(\pi N \mathbf{s} \cdot \mathbf{a}) \approx e^{-\pi(N \mathbf{s} \cdot \mathbf{a})^2}$$

Particle-size broadening

We have not considered the peak width carefully yet. It can be very broad for small nanoparticles, because the distribution of diffraction intensity in reciprocal-space is related to the Fourier transform of the particle shape.

Let's say the scattering vector is $\mathbf{q} = \mathbf{k}' - \mathbf{k} = \mathbf{g} + \mathbf{s}$, where \mathbf{s} is the excitation error and \mathbf{g} is an RLV. For a radial scan, we can say $\mathbf{s} \parallel \mathbf{g} \parallel \mathbf{a}$. Note that this is completely different from TEM, where we assumed $\mathbf{s} \perp \mathbf{g}$. Write $q = 2 \sin \theta / \lambda$, so

$$\frac{dq}{d\theta} = \frac{2 \cos \theta}{\lambda}$$

Now

$$s = \Delta q = \frac{2 \cdot \Delta \theta \cdot \cos \theta}{\lambda}$$

The intensity is a gaussian w.r.t.

$$\mathbf{s} \cdot \mathbf{a} = s \cdot a = \frac{\Delta(2\theta) \cdot \cos \theta}{\lambda} \cdot a$$

So

$$I' = I_{\max} \cdot e^{-\pi \left\{ N \left[\frac{\Delta(2\theta) \cdot \cos \theta}{\lambda} \right] a \right\}^2}$$

Now, let's say our particle size is $L = Na$. Then the FWHM is

$$\frac{1}{2} I_{\max} = I_{\max} \cdot e^{-\pi[L(\pm\Delta\theta)\cos\theta/\lambda]^2}$$

From this, we can estimate the width of the peak in 2θ :

$$\Delta(2\theta) = 2 \cdot (\Delta\theta) = \frac{2\sqrt{\frac{\ln 2}{\pi}} \cdot \lambda}{L \cdot \cos\theta} = \frac{(0.94)\lambda}{L \cdot \cos\theta}$$

Sometimes, this is just written

$$\Delta(2\theta) = \frac{K \cdot \lambda}{L \cdot \cos\theta}$$

where $K \approx 1$. This is called the Scherrer equation.

Temperature factor

If we include thermal motion about the equilibrium positions, a displacement must be included for the position of each atom

$$\rho_m(\mathbf{r}) = \sum_k \rho^{(k)}(\mathbf{r} - \mathbf{d}^{(k)} - \boldsymbol{\delta}^{(k)})$$

But the displacement is a small, random correction, which has no correlations among unit cell separated by more than a few lattice vectors. The entire charge density for the crystal is then

$$\rho(\mathbf{r}) = \lim_{N \rightarrow \infty} \sum_{n=1}^N \sum_k \rho^{(k)}(\mathbf{r} - \mathbf{d}^{(k)} - \boldsymbol{\delta}_n^{(k)})$$

Note that we lack of ideal, long-range periodicity prevents the direct use of the lattice sum. We can compute the total scattering amplitude using

$$\begin{aligned} F(\mathbf{r}^*) &= \mathfrak{T}[\rho(\mathbf{r})] = \lim_{N \rightarrow \infty} \sum_{n=1}^N \sum_k \mathfrak{T}[\rho^{(k)}(\mathbf{r} - \mathbf{r}_n - \mathbf{d}^{(k)} - \boldsymbol{\delta}_n^{(k)})] \\ &= \lim_{N \rightarrow \infty} \sum_{n=1}^N \sum_k f^{(k)}(\mathbf{r}^*) \cdot e^{2\pi i \mathbf{r}^* \cdot (\mathbf{r}_n + \mathbf{d}^{(k)} + \boldsymbol{\delta}_n^{(k)})} \end{aligned}$$

Let's write this simply as

$$F(\mathbf{r}^*) = \sum_k f^{(k)} \cdot e^{2\pi i \mathbf{r}^* \cdot \mathbf{d}^{(k)}} \cdot \sum_n e^{2\pi i \mathbf{r}^* \cdot \mathbf{r}_n} \cdot e^{2\pi i \mathbf{r}^* \cdot \boldsymbol{\delta}_n^{(k)}}$$

with the understanding that $f^{(k)} = f^{(k)}(\mathbf{r}^*)$ and we are interested in the limit of an infinite lattice. The $\boldsymbol{\delta}_n^{(k)}$ are not static values, but, rather, fluctuate randomly about $\mathbf{0}$. A diffraction experiment samples the time-average of $F(\mathbf{r}^*)$ on a temporal scale much longer than the thermal motion.

$$\langle F(\mathbf{r}^*) \rangle = \left\langle \sum_k f^{(k)} \cdot e^{2\pi i \mathbf{r}^* \cdot \mathbf{d}^{(k)}} \cdot \sum_n e^{2\pi i \mathbf{r}^* \cdot \mathbf{r}_n} \cdot e^{2\pi i \mathbf{r}^* \cdot \boldsymbol{\delta}_n^{(k)}} \right\rangle$$

We define the quantities

$$a^{(k)} = f^{(k)} \cdot e^{2\pi i \mathbf{r}^* \cdot \mathbf{d}^{(k)}}, \quad \phi_n = 2\pi \mathbf{r}^* \cdot \mathbf{r}_n, \quad \text{and} \quad \theta_n^{(k)} = 2\pi \mathbf{r}^* \cdot \boldsymbol{\delta}_n^{(k)}$$

to obtain

$$\langle F(\mathbf{r}^*) \rangle = \left\langle \sum_k a^{(k)} \cdot \sum_n e^{i\phi_n} \cdot e^{i\theta_n^{(k)}} \right\rangle$$

Time averages can be represented as integrals over normalized probability distributions $P^{(k)}(\theta_n^{(k)})$, i.e.,

$$\begin{aligned} \langle F(\mathbf{r}^*) \rangle &= \int_{\theta_1^{(1)}} d\theta_1^{(1)} \cdot P^{(1)}(\theta_1^{(1)}) \cdot \int_{\theta_2^{(1)}} d\theta_2^{(1)} \cdot P^{(1)}(\theta_2^{(1)}) \dots \\ &\quad \cdot \int_{\theta_1^{(2)}} d\theta_1^{(2)} \cdot P^{(2)}(\theta_1^{(2)}) \cdot \int_{\theta_2^{(2)}} d\theta_2^{(2)} \cdot P^{(2)}(\theta_2^{(2)}) \dots \\ &\quad \{ e^{i\phi_1} \cdot [a^{(1)} e^{i\theta_1^{(1)}} + a^{(2)} e^{i\theta_1^{(2)}} + \dots] + e^{i\phi_2} \cdot [a^{(1)} e^{i\theta_2^{(1)}} + a^{(2)} e^{i\theta_2^{(2)}} + \dots] + \dots \} \end{aligned}$$

Applying the integrals to only the appropriate terms results in

$$\begin{aligned} \langle F(\mathbf{r}^*) \rangle &= \sum_k a^{(k)} \cdot \sum_n e^{i\phi_n} \cdot \int_{\theta_n^{(k)}} d\theta_n^{(k)} \cdot P^{(k)}(\theta_n^{(k)}) \cdot e^{i\theta_n^{(k)}} \\ &= \sum_k a^{(k)} \cdot \sum_n e^{i\phi_n} \cdot \langle e^{i\theta_n^{(k)}} \rangle \end{aligned}$$

We expect no correlations in the thermal motions of atoms beyond, perhaps, nearest neighbors, so the reference to unit cell can be eliminated from the time average

$$\langle F(\mathbf{r}^*) \rangle = \sum_k a^{(k)} \cdot \langle e^{i\theta^{(k)}} \rangle \cdot \sum_n e^{i\phi_n}$$

We can expand the exponent of each time-average term in a Taylor's series. Using $x = \theta^{(k)}$, we have

$$e^{ix} = 1 + ix + \frac{1}{2}(ix)^2 + \frac{1}{6}(ix)^3 + \dots = 1 + ix - \frac{1}{2}x^2 - \frac{i}{6}x^3 + \dots$$

The time average is

$$\langle e^{ix} \rangle = 1 + i\langle x \rangle - \frac{1}{2}\langle x^2 \rangle - \frac{i}{6}\langle x^3 \rangle + \dots$$

If the probability distributions are symmetric about 0, then the odd-powered terms vanish. Including only the lowest-order correction, this gives

$$\langle e^{ix} \rangle \approx 1 - \frac{1}{2}\langle x^2 \rangle$$

Notice that expansion of a gaussian distribution gives the same lowest-order correction

$$\langle e^{-x^2/2} \rangle \approx 1 - \frac{1}{2}\langle x^2 \rangle$$

Thus

$$\langle e^{i\theta^{(k)}} \rangle \approx \left\langle e^{-(\theta^{(k)})^2/2} \right\rangle$$

Crystallography & Structure of Nanomaterials

The exponent of the time-averaged terms involve only the component of displacement along \mathbf{r}^* . We abbreviate $u^{(k)} = \mathbf{r}^* \cdot \boldsymbol{\delta}^{(k)}$, and substitute the Gaussian form, giving

$$\langle e^{2\pi i u^{(k)}} \rangle \approx e^{-2\pi^2 \langle (u^{(k)})^2 \rangle}$$

Recognizing that $r^* = 2 \sin \theta / \lambda$, this exponential term for each atom in the unit cell is called the Debye-Waller factor, which contains the dependence on temperature T

$$e^{-2\pi^2 \langle (u^{(k)})^2 \rangle} = e^{-M^{(k)}(\theta, T)}$$

The lattice sum is unchanged, indicating that we can write the scattering amplitude as

$$F(\mathbf{r}^*, T) = \langle F(\mathbf{r}^*) \rangle = \frac{1}{V} \cdot \sum_{\mathbf{H}} F_{\mathbf{H}}(T) \cdot \Delta(\mathbf{r}^* - \mathbf{r}_{\mathbf{H}}^*)$$

where

$$F_{\mathbf{H}}(T) = \sum_k f^{(k)} \cdot e^{-M^{(k)}(\theta_{\mathbf{H}}, T)} \cdot e^{2\pi i \mathbf{H} \cdot \mathbf{X}^{(k)}}$$

Using these observations

$$I_{\mathbf{H}}(T) \propto \left| \sum_k f^{(k)} \cdot e^{-M^{(k)}(\theta_{\mathbf{H}}, T)} \cdot e^{2\pi i \mathbf{H} \cdot \mathbf{d}^{(k)}} \right|^2$$

The net effect is to replace the atomic form factors in the structure factor sum with damped forms

$$f^{(k)} \rightarrow f^{(k)} \cdot e^{-M^{(k)}(\theta_{\mathbf{H}})}$$

Thus, the primary effect of elevated temperature is not to broaden the reflections, but rather to reduce their intensities. The structure factors can be computed as

$$F_{\mathbf{H}}(T) = \sum_k f^{(k)} \cdot e^{-M^{(k)}(\theta_{\mathbf{H}})} \cdot e^{2\pi i \mathbf{H} \cdot \mathbf{X}^{(k)}}$$

The assumption that $\sum_n e^{i\phi_n} \cdot \langle e^{i\theta_n^{(k)}} \rangle = \langle e^{i\theta^{(k)}} \rangle \cdot \sum_n e^{i\phi_n}$ is not precise, due to correlated motion among neighboring cells and, ultimately, long-range crystal vibrations, i.e., phonons. The result is a continuous background in the diffracted intensity that increases with temperature and scattering angle.

Simplified derivation

Alternatively, we can take the approach of assuming each atom in the unit cell is delocalized by the distribution $P^{(k)}(\delta)$

$$P^{(k)}(\delta) = \frac{1}{R^{(k)} \cdot \sqrt{2\pi}} \cdot e^{-\delta^2 / 2(R^{(k)})^2}$$

such that

$$R^{(k)} = \sqrt{\langle (\delta^{(k)})^2 \rangle}$$

Crystallography & Structure of Nanomaterials

is the root-mean-squared displacement, with typical room temperature values $R^{(k)} \approx 0.005 - 0.020$ nm.

We consider the electron concentration of each atom in the unit cell to be altered by thermal motion as

$$\rho_{\text{th}}^{(k)}(r) = \int_{r'=-\infty}^{\infty} dr' \cdot \rho^{(k)}(r-r') \cdot P^{(k)}(r') = \rho^{(k)}(r) * P^{(k)}(r)$$

That effective structure factor at finite temperature is

$$F(\mathbf{r}^*, T) = \mathfrak{S}[\rho_{\text{th}}(\mathbf{r})] = \lim_{N \rightarrow \infty} \sum_{n=1}^N \sum_k \mathfrak{S}[\rho_{\text{th}}^{(k)}(\mathbf{r} - \mathbf{r}_n - \mathbf{d}^{(k)})]$$

At an some non-zero temperature, using the convolution theorem, the atomic scattering amplitude is

$$f_{\text{th}}^{(k)}(r^*) = \mathfrak{S}[\rho_{\text{th}}^{(k)}(r)] = \mathfrak{S}[\rho^{(k)}(r)] \cdot \mathfrak{S}[P(r)]$$

The form factors $f^{(k)}(r^*)$ of the atoms without thermal motion were discussed previously. The Fourier transform of the probability distribution is the Debye-Waller factor

$$\mathfrak{S}[P^{(k)}(r)] = e^{-2\pi^2(r^* \cdot R^{(k)})^2} = e^{-M^{(k)}(\theta)}$$

where we again recognize that $r^* = 2 \sin \theta / \lambda$.

$$f_{\text{th}}^{(k)}(r^*) = f^{(k)}(r^*) \cdot e^{-M^{(k)}(\theta)}$$

The exponents of the Debye-Waller temperature factors contain the terms

$$M^{(k)}(\theta) = 8\pi^2 \cdot (\sin \theta \cdot R^{(k)} / \lambda)^2$$

This analysis gives the same expression as the previous, microscopic description for the influences of thermal motion on structure factors, but does not lead to a mechanism for the thermal diffuse scattering

$$F_{\text{H}}(T) = \sum_k f^{(k)} \cdot e^{-M^{(k)}(\theta_{\text{H}})} \cdot e^{2\pi i \bar{\mathbf{H}} \cdot \mathbf{X}^{(k)}}$$